sustainability

Article

Multi-Risk Assessment in the Veneto Region: An Approach to Rank Seismic and Flood Risk

Gabriella Tocchi [1,*], Daria Ottonelli [2], Nicola Rebora [2] and Maria Polese [1]

[1] Department of Structures for Engineering and Architecture, University of Naples Federico II, Via Claudio 21, 80125 Naples, Italy
[2] CIMA Research Foundation, Via A. Magliotto 2, 17100 Savona, Italy
* Correspondence: gabriella.tocchi@unina.it

Abstract: Effective disaster risk management in a given area relies on the analysis of all relevant risks potentially affecting it. A proper multi-risk evaluation requires the ranking of analyzed risks and the estimation of overall expected impacts, considering possible hazards (and vulnerabilities) interactions as well. Due to their complex and challenging modelling, such interactions are usually neglected, and the analysis of risks derived from different sources are commonly performed through independent analysis. However, often the assessment procedures adopted for the analysis as well as the metrics used to express various risks are different, making results of single risk analyses hardly comparable. To overcome this issue, an approach that allows for comparing and ranking risks is presented in this study. The approach is demonstrated through an application for an Italian region. Earthquakes and floods are the investigated hazards. First, in order to select the case study area, the municipalities within the Veneto region where both risks could be highest are identified by adopting an index-based approach. Then, the harmonization of seismic and flood risk assessment procedure is performed. Sub-municipal areas are selected as scale of analysis and direct economic losses are chosen as common impact metrics. The results of the single risk analyses are compared using risk curves as standardization tool. The EAL (expected annual losses) are estimated through risk curves and the ratios between EAL due to floods and earthquakes are mapped, showing in which area risk is significantly higher than the other.

Keywords: seismic risk; flood risk; multi-risk assessment; losses comparison

Citation: Tocchi, G.; Ottonelli, D.; Rebora, N.; Polese, M. Multi-Risk Assessment in the Veneto Region: An Approach to Rank Seismic and Flood Risk. *Sustainability* **2023**, *15*, 12458. https://doi.org/10.3390/su151612458

Academic Editor: Michalis Diakakis

Received: 26 June 2023
Revised: 28 July 2023
Accepted: 7 August 2023
Published: 16 August 2023

1. Introduction

Understanding the potential impacts of natural hazards plays a crucial role for effective disaster risk management. Risk assessment consists in determining the nature and extent of disaster risk by analyzing potential hazards and evaluating existing conditions of exposure and vulnerability [1]. Although, to date, risk assessment predominantly focuses on a single hazard [2,3], events occurred during past decades showed that natural-hazard disasters frequently spatially and temporally overlap [4–7]. A hazardous event may trigger another, such as when an earthquake triggers a tsunami or a landslide. These kinds of hazard interactions are usually called cascades [8–10] or domino effects [11–13]. Multiple hazards may also occur at the same time because they are triggered by the same triggering event (e.g., storm surge and flooding occurring during a hurricane). They are often referred to as coupled events or concurrent hazards [14,15]. Nevertheless, impacts of an event can change the characteristics of exposed physical elements, making them more vulnerable to other hazards that may subsequently occur. This means that potential impacts caused by different risk sources may be much greater than the sum of the single parts when considering their relationships and dependencies.

For a rigorous multi-hazard risk assessment all possible risk interactions (both at the level of hazard and of vulnerability) should be considered. However, modelling such interactions is still challenging as it requires a deep investigation of possible chains of events and the estimation of the related probability of occurrence [16–19]. A straightforward approach to perform a quantitative multi-risk analysis is the so-called multi-layer single risk assessment [20]. It consists in analyzing two or more risks ignoring their possible interactions but harmonizing the assessment procedures to make them comparable. Indeed, methodologies and spatial/temporal resolution adopted for the analysis as well as metrics used for measuring expected losses from natural hazards may differ. Thus, to make risks generated from different perils comparable it is necessary to (1) harmonize the assessment procedure and (2) adopt suitable standardization schemes for impacts evaluation. Despite potential hazards interaction and cascading effects being neglected, this approach allows for ranking the different risks potentially affecting a given region, representing a prominent tool for supporting decision makers in defining appropriate risk mitigation strategies.

In this study an approach for integrated multi-hazard risk assessment is proposed. Adopting a methodology developed within EU project BORIS (cross border risk assessment for increased prevention and preparedness in Europe, GA n. 101004882) and presented elsewhere [21], this paper proposes the application of a multi-layer single hazard framework for analyzing and comparing seismic and flood risks. The harmonization procedure and the results comparison are demonstrated for some municipalities in the Veneto region, Italy. This region is chosen as being potentially prone to multi-hazard effects, due to its high seismicity and the frequent overflowing of river network during heavy rain events. Sub-municipal areas are selected as scale of analysis and a downscaling procedure is proposed for modelling the exposure using easily available data at larger scale. Residential buildings are considered as assets at risk and impacts are estimated in terms of direct economic losses. The comparison between the two perils is shown through risk maps and risk curves. The maps provide risk rankings and allow for identifying areas where one risk is predominant. The risk curves allow for comparing expected losses (according to a predefined metric, e.g., economic losses) due to floods and earthquakes that potentially affect the territory.

2. Materials and Methods

The approach proposed in this study is composed of two complementary steps. First, a preliminary and semi-quantitative assessment is performed to identify areas where potential negative consequences of considered risks could be highest. To this aim, an index-based approach is adopted, i.e., a process where risk originated from the different hazards involved is expressed by a dimensionless number (an index), and it is calculated through the aggregation of several normalized sub-indicators. A detailed description of the approach adopted can be found in the following section (Section 2.1). The municipal scale is the territorial unit of analysis considered in this first step. The identification of the riskiest municipalities in the region (i.e., where the defined multi-risk index is highest) leads the selection of case study for the performing of a detailed quantitative multi-risk assessment at sub-municipal scale (the second step of the proposed procedure). Specifically, expected losses due to multiple hazards in the study area are estimated by adopting the multi-layer single risk assessment methodology proposed in BORIS, as described in Section 2.2. The BORIS project, finalized in December 2022, was aimed at the development of a harmonized multi-risk assessment in cross-border areas, with particular focus on seismic and flood risk in the Eastern Alps transboundary region (Italian—Slovenian—Austrian borders). Evidence demonstrates that most economic losses in Italy from disasters during the last decades were caused by earthquakes and floods [22]. Earthquakes are also one of the natural hazards causing more significant impacts in terms of deaths, only behind extreme temperatures (i.e., heat waves) that are responsible for the larger number of casualties. Thus, without claiming to compare all hazards potentially affecting an area, but with the aim to demonstrate the methodology for multi-layer single risk assessment proposed in BORIS, these two risks (seismic and flood) are the only ones considered in this study.

The methodology proposed herein is meant to be a procedure to support decision makers to formulate prevention and mitigation strategies and to allocate available resources. As a matter of fact, comparing and ranking seismic and flood risks would allow for identifying the predominant risk in a given area and to understand which kinds of mitigation actions should be prioritized to reduce risk to an acceptable level. Although multi-risk analysis may not be as suitable for designing structural risk mitigation solutions for isolated threats, accounting for more than one hazard in risk analysis could be useful to avoid potential unwanted effects of disaster risk reduction measures implemented to decrease the risk of a single hazard type on risk induced by other hazards. These potentially negative effects between measures are defined by [23] as "asynergies". Furthermore, even if the two hazards analyzed may be considered as independent (i.e., no hazard interactions) [15], multi-layer single risk assessment allows for obtaining a measure of the overall level of risk attained when such hazards occurred within a short space of time, which could be useful for insurance pricing as well.

2.1. Case Study Selection

The selection of case study for this application is performed by adopting the approach proposed in [24], that allows for prioritizing areas exposed to multiple risks through the definition of a risk index (RI). For each risk analyzed, individual normalized indicators representative of risk components (i.e., hazard, vulnerability, exposure) are defined at municipal scale. For each municipality investigated, such indicators are aggregated in order to obtain an overall risk score (i.e., RI) that represents (for the considered municipality) the level of potential impacts due to multiple hazards. Specifically, two natural hazards are taken into account in applying the proposed tool: earthquake and flood.

For seismic hazard, the value of peak ground acceleration (PGA) at municipal centroid for a probability of exceedance of 10% in 50 years (i.e., a return period of 475 years) is selected as hazard indicator. This value is derived from the official reference for seismic hazard values of Italy, i.e., the map of seismic hazard also known as MPS04 (seismic hazard model, "Modello di pericolosità sismica" in Italian, developed in 2004 and proposed by [25,26]). The seismic physical vulnerability indicator is defined according to the index-based approach presented in [27]. A vulnerability index (VI) for buildings is calculated based on their features, such as the construction material and the structural system (e.g., irregular layout or regular layout masonry structure, reinforced concrete (RC) frame or walls), the type of design for RC buildings and the type of horizontal structures for masonry ones. The VI assumes value between 0 and 1 and its value is associated with the seismic performance of buildings (e.g., values close to 0 indicate high seismic performance, values close to 1 poor seismic performance). The physical vulnerability indicator is given by the VI at municipal level, calculated by accounting for the distribution of buildings in several classes (each class is associated with a range of VI values).

Concerning flood risk, the hazard indicator is defined as the percentage of expected flooded area in a given municipality, according to a medium probability scenario map (return period between 100 and 200 years), derived from ISPRA ("Istituto Superiore per la Protezione e la Ricerca Ambientale" in Italian), a public research institute that provides services for the Italian Ministry for Environment, Land and Sea Protection (www.isprambiente.gov.it, accessed on 9 August 2022). The flood physical vulnerability indicator is estimated as the percentages of buildings with only one storey within the municipality, and as such, typology is the most vulnerable one according to several flood vulnerability models [28–30]. It is worth mentioning that physical exposure is considered and included in the definition of seismic physical vulnerability (as the definition of VI at municipal level requires information on building inventory) and in the definition of flood hazard (i.e., the spatial distribution of buildings within a municipality is assumed uniform so that the inundated area is also representative of the proportion of potentially inundated buildings). In [24], an indicator representative of the social vulnerability of the residential population and one representative of the exposed population is also defined. However, this component is ignored herein as this study focuses on multi-risk assessment of physical assets and aims to compare the risks in terms of economic losses.

The individual indicators defined are first normalized (transformed in dimensionless, pure numbers) through their empirical cumulative distribution functions (ECDFs), and then aggregated. ECDFs express the probability that a random variable X will take a value less than or equal to a given value x. For example, in terms of the seismic hazard indicator, X is the value of PGA for the selected municipalities and the selected return. The *RI* value at municipal level is calculated as follows:

$$RI_j = [F_h^s(h_j) \cdot F_{Pv}^s(v_j)]^{w_s} \cdot [F_h^f(h_j) \cdot F_{Pv}^f(v_j)]^{w_f} \tag{1}$$

where ${F_h}^s(h_j)$, ${F_{Pv}}^s(v_j)$, ${F_h}^f(h_j)$ and ${F_{Pv}}^f(v_j)$ are the ECDF values of the seismic hazard, seismic physical vulnerability, flood hazard and flood physical vulnerability, respectively, evaluated at municipality *j*. w_s and w_f are the weights adopted for seismic and flood risk, representing the relative importance of multi-risk measuring. Ideally, such weights should be defined by stakeholders based on their objectives and their knowledge of the territory. With the aim to give a measure of the overall level of risk (due to both seismic and flood) and refer to the detailed assessment of the evaluation of relative importance of the two risks in each municipality, in this application the two weights are considered equal (w_s = w_f = 0.5), i.e., seismic and flood risk are assumed to have the same importance.

The approach presented above is applied to all municipalities in the Veneto region. Its use allows for selection of municipalities in the region presenting high flood risk/seismic risk or for which both risks are significant. For instance, Portobuffolè is the town with the highest RI in the whole region (RI = 0.69), representing 40% of the municipal area potentially inundated by events with average probability of occurrence (i.e., return period 100–200 years), high flood vulnerability according to the adopted criteria (i.e., high percentage of buildings with only one story) and significant seismic hazard as well. Despite the town of Salgareda presenting the highest flood hazard indicator (98% of potentially flooded area) and high flood vulnerability indicator (about 30% of buildings with one story against the 17% of Portobuffolè), the hazard seismic indicator in Portobuffolè is higher (PGA = 0.16 g for the considered return period against PGA = 0.11 g of Salgareda) and this leads to a lower (but still relevant) RI value for the former one (RI = 0.59). Similarly, Nervesa della Battaglia shows very high seismic hazard (PGA = 0.22 g) and a significant seismic physical vulnerability, thus, even if only 14% of the municipality is expected to be inundated, the RI obtained for this city is quite high as well (RI = 0.53).

Figure 1 shows the map of RI for the region investigated and the municipalities selected for the application proposed herein. The selected case study area comprises 25 municipalities close to the town with the highest RI (Portobuffolè), including the ones previously mentioned (Salagareda and Nervesa della Battaglia). Despite RI also assuming high values in other municipalities on the west side (Brentino Belluno, RI = 0.63; Bardolino, RI = 057) and the northern side of the region (Longarone, RI = 0.57; Ospitale di Cadone, RI = 0.57), the area close to Portobuffolè (Figure 1b) is selected as the case study because it encompasses towns with very different values of seismic and flood hazard inputs. As a matter of fact, many municipalities close to the city of Brentino Belluno (west side) are characterized by a medium–high seismic hazard (PGA = 0.16 g almost everywhere in the area) while the flood hazard indicator is only significantly high for the cities of Bardolino and Torri del Benaco (percentage of expected flooded area within the municipality greater than 70%). Municipalities close to Longarone (northern side) show very high values for seismic hazards (PGA greater than 0.19 g), while flood hazard is not relevant at all in this area (percentage of expected flooded area within the municipality is lower than 10%). On the contrary, the defined study area includes both municipalities with medium (e.g., Zeson di Piave, PGA = 0.10 g), high (e.g., Spresiano, PGA = 0.18 g) and very high (e.g., Crocetta del Montello, PGA = 0.23 g) seismic hazard and municipalities from medium to high flood hazard due to the presence of the Piave river (e.g., Sernaglia della Battaglia and Ponte di Piave, where the percentages of municipal areas expected to be inundated are 30% and 78%, respectively). Such variation of input values would allow for covering larger ranges of seismic and flood risk values and help in demonstrating the usefulness of the proposed approach for comparing risks.

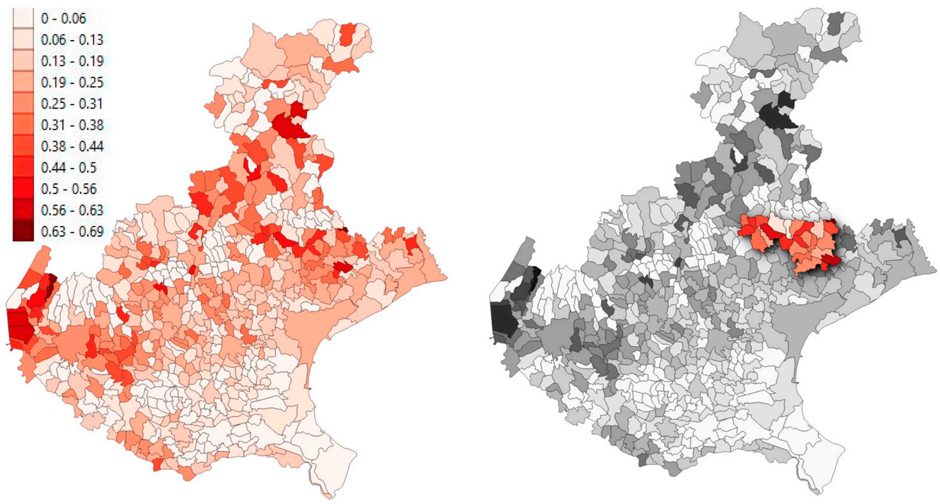

(**a**) (**b**)

Figure 1. RI map of the Veneto region (**a**) and municipalities selected as the case study (**b**).

2.2. Multi-Risk Assessment

As mentioned before, the main problem that arises for the application of the multi-layer single risk approach is the comparability of the different risks. As a matter of fact, different hazards often require a different scale of analysis as the extent of the area impacted by diverse hazards can greatly vary. For instance, seismic risk is often assessed at large scale (e.g., regional, municipal), while flood analysis usually requires a smaller scale as flood hazard varies spatially much more with respect to seismic hazard. Furthermore, floods are typically more frequent than earthquakes, that means that the former are characterized by very short return periods (the average time of occurrence between events of a given magnitude) while the second by long or very long return periods. Accordingly, metrics commonly used to measure impacts are also very different and may be not directly comparable. Thus, the harmonization of risks assessment is crucial to allow for their comparison.

The first step towards a harmonized assessment is the selection of the type of analysis (i.e., probabilistic or scenario-based) and a common risk time frame (i.e., the time—generally expressed in years—during which a risk, if it occurs, will impact). As the main objective of this study is a better understanding of risks potentially affecting the area and it is mostly aimed at prevention purposes, a probabilistic risk assessment is performed herein. The evaluation of the risk arises from the convolution of three main components: hazard, (physical) vulnerability and exposure. Hazard expresses the probability of exceedance of the intensity measure level in a certain interval of time at a site, and it can be represented through hazard maps or hazard curves. As intensity measure, the PGA at municipal centroid is adopted for seismic risk analysis and the water depth (expressed in meters) for flood risk. Vulnerability models express the propensity of buildings to be damaged as a function of the selected intensity measures (i.e., PGA and water depth). The exposure gives the distribution within the unit of analysis of buildings in classes, defined based on the related typological and structural features relevant for describing the (seismic and flood) vulnerability. As no interactions at hazard or vulnerability level are considered, different classification rules could be adopted for modelling the exposed buildings to floods and earthquakes. Furthermore, geographic units adopted for the analysis can be different, provided that the results are finally added up and compared with reference to the same territorial scale. Therefore, flood risk assessment is first performed at building level; then, results are aggregated at larger scale, namely, the scale of analysis adopted for seismic risk (the sub-municipal areas described in Section 2.2.2).

The risk time frame is set to one year and impacts are estimated as the amount of losses expected annually for a given community. Economic losses and people affected (casualties, injured and homeless) are the most commonly used metrics for expressing risk [31]. However, it should be noted that direct economic losses are mostly related to buildings' structural damages (i.e., reconstruction costs) after earthquakes, whereas in case of flood, replacement costs of existing household goods could be equally (if not more) relevant to structural repair costs. Furthermore, people affected by a flood are usually estimated as the totality of people located in the inundated area. Indeed, flooded roadways (and not only buildings) may also cause deaths, injuries or displaced households. Thus, unlike earthquakes, people affected cannot be estimated only by accounting for residents in severe damaged or collapsed buildings. For this reason, in this study the comparison between risks is performed only in terms of direct economic losses referred to buildings' structural damages.

Most commonly used standardization procedures for comparing different risks are risk matrices, risk indices and risk curves. Risk matrices present a risk in a matrix-system, illustrating the hazard likelihood on one axis and its potential impact on the other [32]. The combinations of consequence and likelihood are mapped into a limited number of risk categories (e.g., extreme, high, medium, low), often visualized by different colors. They were successfully used in multi-risk studies, as they allow for graphically representing several hazards in a unique matrix by being located in the appropriate section of the matrix space (i.e., based on the related likelihood and potential impacts) [33,34]. However, they are often criticized due to the subjectivity and/or lack of transparency of certain choices such as the scoring or coloring of the risk matrix that expresses subjective risk perceptions [35]. Risk indices express potential impacts of hazards through a dimensionless number, obtained as a combination of sub-indicators representative of each risk component, as also shown in Section 2.1. Although they are a straightforward tool to compare two or more risks, index-based approaches only give a semi-quantitative measure of risk level and do not allow a proper quantification of expected losses. On the contrary, risk curves allow for quantifying risk induced by natural hazards as they are the usual outcomes from a fully probabilistic approach. Risk curves, also called loss exceedance curves, relate the mean annual frequency of exceedance of a given hazardous event to the corresponding loss metric selected (e.g., direct economic losses). The calculation of risk in a given period is a conditional relation of hazard and vulnerability to the exposed elements [36,37]. Considering all possible hazard events, defined by different intensity and frequency (i.e., hazard curves or hazard maps), a fully probabilistic risk estimation can be performed using the following equation [38]:

$$v(p) = \sum_{i=1}^{Events} \Pr(P > p|\, Event_i)\, F_A(Event_i) \tag{2}$$

where $v(p)$ is the exceedance rate of loss p; F_A ($\mathrm{Event_i}$) is the annual frequency of occurrence of $Event_i$; and Pr ($P > p \mid Event_i$) is the probability of the loss to be greater than or equal to p, conditioned by the occurrence of $Event_i$. The graphical representation of $v(p)$ is the risk curve. A commonly used risk metric is the "Average Annual Loss" (AAL), i.e., the weighted average of all plausible loss values calculated as an area under the risk curve (Equation (3)). This value is also called "Expected Annual Losses" (EAL).

$$AAL = \int_0^\infty v(p)dp \tag{3}$$

As exceedance probabilities are not expressed in a hazard-specific unit, losses among different hazards are directly comparable through risk curves. Examples of the use of risk curves for comparing and ranking different risks can be found in [39–41]. Therefore, risk curves can be considered the most suitable tool for a quantitative assessment of single-hazard risks towards their consistent comparison. For this reason, they were adopted as standardization tool in BORIS [41] and they are used in this study as well.

Figure 2 shows the main steps of the methodology adopted herein to perform multi-layer single risk assessment. Each step is represented by green dashed boxes. In the hazard evaluation step, the seismic and flood hazard models to be used as input for the assessment are selected. The exposure assessment involves the definition of the characteristics and the amount of exposure elements and their spatial distribution along the analyzed territory. In this phase it is necessary to also define the asset at risk considered in the analysis and the spatial scale to adopt for single risk assessments. As mentioned before, the spatial scale adopted for seismic and flood risk could differ, but the results should finally be aggregated at the same scale to allow risks comparison. On the contrary, the asset at risk must be the same. The vulnerability modelling consists in defining the fragility/vulnerability curves to adopt for the estimation of expected damages and losses related to the considered asset at risk. The impact estimation (phase) allows the evaluation of losses with the use of suitable consequence functions. Impacts (i.e., direct economic losses) are estimated with reference to several events with a given annual frequency of occurrence. In other words, the impact estimation is performed several times using the map providing the spatial distribution of expected hazard intensity at defined mean annual frequency of exceedance as input each time. Each value of (direct) economic losses calculated for a specific event (hazard intensity associated with a specific return period) represents a point of the risk curve. Once the risk curves are built, the value of EAL is calculated and risk comparison is performed. In the figure, the requirements for ensure risk comparability are reported in orange. For instance, for a consistent seismic and flood impact estimation, it is necessary to adopt the same risk metrics, e.g., direct economic losses due to buildings' structural damage. Furthermore, adopting the same unit costs for such buildings is needed, i.e., the same repair or reconstruction costs. In the following sections, models and data adopted in each step of the analysis are presented.

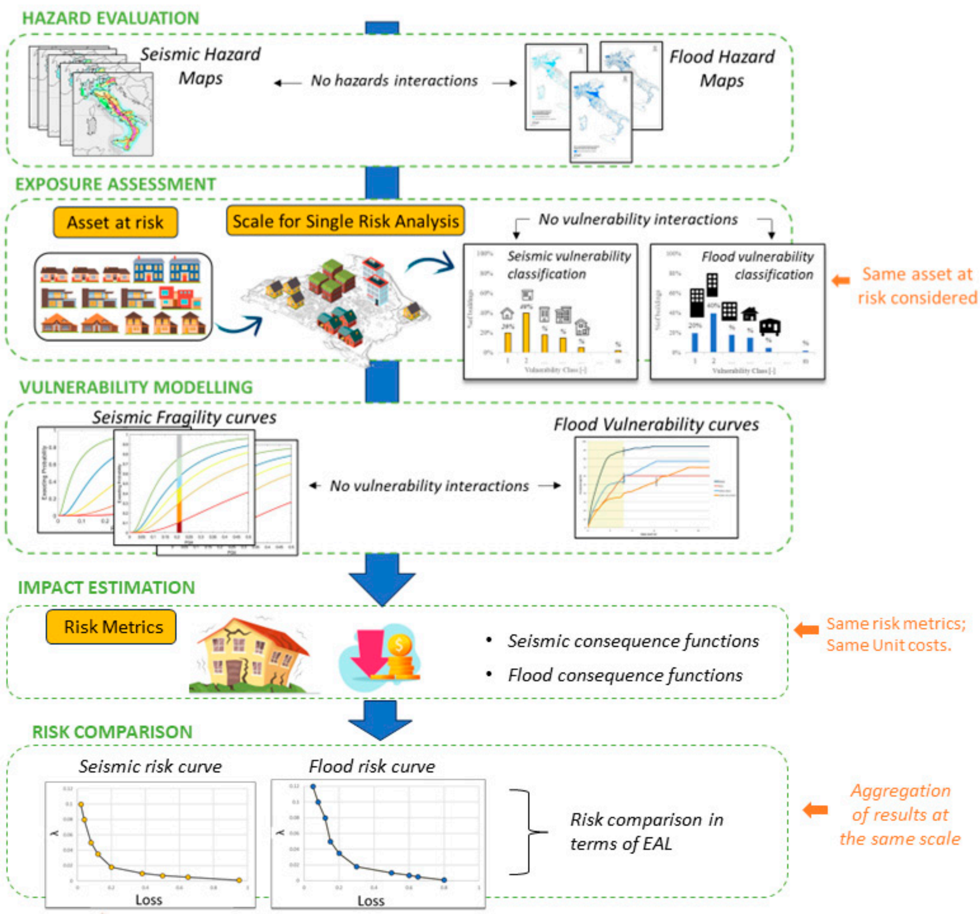

Figure 2. Steps of the proposed methodology for multi-risk comparison and ranking.

2.2.1. Hazard Evaluation

The MPS04 model is used as seismic hazard input. Nine hazard maps corresponding to nine different probabilities of exceedance of the ground motion intensity in 50 years (2%, 5%, 10%, 22%, 30%, 39%, 50%, 63%, 81%) are derived from PSHA (probabilistic seismic hazard analysis) [26]. These maps report the values of maximum horizontal component of the expected ground shaking (ag = fraction of gravity acceleration) referred to rock soils (i.e., PGA) for the different return periods considered over a grid of more than 16,000 points. The step of the grid points is of 0.05 degrees. This resolution is not suitable for assessing seismic hazards at small scale (e.g., sub-municipal areas). Therefore, PGA at the municipal centroid is considered as the seismic hazard input for the analysis. It is estimated through the distance-weighted average of the closest grid point values [42]. On the contrary, possible local amplification effects can be evaluated at lower scale. More specifically, for each sub-municipal unit of analysis, the value of PGA at the municipal centroid is amplified accounting for soil factors, estimated using the Italian Vs30 maps proposed in [43]. It is worth mentioning that the set of yearly exceedance probabilities covered by the model may be insufficient for a time-based risk assessment. Therefore, interpolation and extrapolation of the hazard curves are performed herein. Specifically, linear interpolation in the logarithmic domain is performed to obtain the seismic intensity for low return periods (i.e., PGA values expected for 20-year return period event, neglecting the effects of more frequent events with very low intensity) while extrapolation is adopted for high return periods (i.e., 5000 years), where the "low" and "high" return periods indicate, respectively, return periods much lower and much higher that the return period typically used in structural design.

For the flood risk assessment, the area of interest is the hydrological basin of the Piave river. The Piave River is a large catchment (area = 4.127 km^2) situated in northeastern Italy, which starts in the Alps in the Friuli-Venezia-Giulia Region and runs through the Veneto Region to the Adriatic Sea.

Starting from the EU Floods Directive 2007/60/EC maps of flood extent available for the Veneto Region, the CIMA Research Foundation has produced flood hazard maps also reporting expected water levels of an area flooded in three scenarios where flood extent was available: (1) a high probability scenario (a return period of 25 years), see Figure 3a, (2) a medium probability scenario (a return period of 100 years) and (3) a low probability scenario or extreme event (a return period of 300 years), see Figure 3b. In order to build hazard maps that can provide flood extent and depth with a timestep of one year from 30 years to 300 years, an interpolation technique of the existing flood maps technique was applied [44].

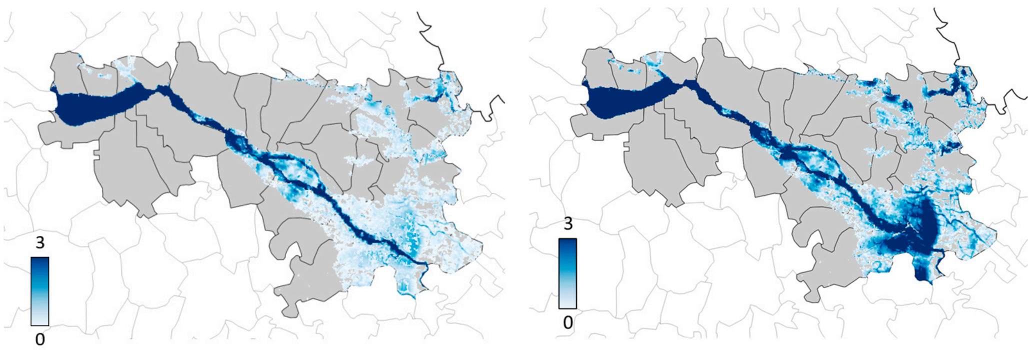

(**a**) (**b**)

Figure 3. Water depth flood hazard map of the municipalities selected: (**a**) considering an event with a return period of 25 years; (**b**) with a return period of 300 years. The range of water depth is limited from 0 to 3 m. Source: CIMA Research Foundation.

2.2.2. Exposure Information

In the risk equation, the exposure model estimates "the situation of people, infrastructure, housing, production capacities and other tangible human assets located in hazard-prone areas" [45]. The identification of elements at risk regarding their quantity, spatialization, vulnerability characteristics and value is assessed through an exposure analysis. It covers several dimensions, for example, the physical (e.g., building stock and infrastructure), the social (e.g., humans and communities) and the economic dimensions [46]. The construction of the exposure model is a function of several aspects: (i) the purposes and scales of the risk analysis, in particular the scale need to be correlated to the other components of the risk equation, above all the spatial resolution of the hazard; and (ii) the integration of data available or directly derived for the specific analysis through appropriate surveys. All these elements contribute to defining the characteristic and granularity of exposure.

The present work considers the physical dimension, developing an exposure model for flood and seismic risks of residential buildings and people associated with them, aimed at multi-layer single risk assessment. For these reasons, an effort is made to define the exposure as homogeneously and consistently as possible for both risks, starting from the same type of data. Several sources can be used to compile inventory for buildings, such as censuses, real-estate registers, building-by-building surveys or remote sensing detections. A census is particularly suitable for large-scale applications (as the present work) as this database is publicly available and covers the whole country. Therefore, exposure models derived for both risks are based on such data. Furthermore, concerning the scale of the exposure, the two risks behave differently. For the flood risk, there is a tendency to create a built-up exposure model as well as possible (also reaching the scale of buildings for territorial risk analysis) to capture a more coherent integration with the flooded area of the hazard map, whereas for the seismic risk, exposure data can be aggregated at different scales according to the availability of hazard information. For instance, the seismic hazard model adopted in Italy (MPS04) provides the values of seismic actions for each point of a 5×5 km mesh covering the whole Italian territory, so the municipality is often selected as the territorial unit of analysis in large scale risk assessment [47]. In order to select a spatial scale of analysis suitable for both risks, sub-municipal areas are identified as the units of analysis. For the delimitation of such zones, information provided by the real estate observatory are adopted. Specifically, the OMI (Osservatorio del Mercato Immobiliare—in Italian) identifies homogeneous municipal areas based on maximum/minimum market and lease real estate values, type of property and state of conservation. Each OMI zone is identified by an alphanumeric code that categorizes areas as central (B), semi-central (C), peripheral (D), suburban (E) and extra-urban (R). Figure 4 shows the delimitation of OMI zones for the city of Oderzo, one of the towns in the case study area.

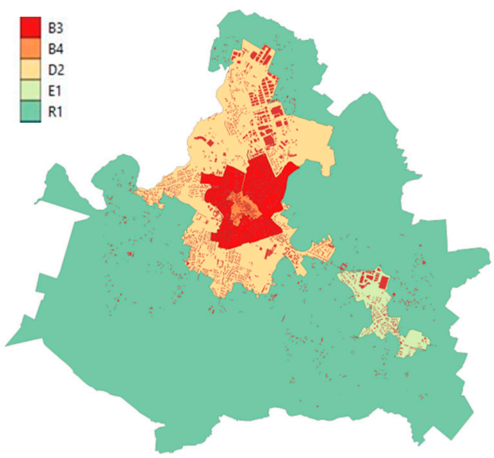

Figure 4. OMI zones for the municipality of Oderzo.

As mentioned before, census data are used to evaluate the type and the amount of assets exposed at risk, i.e., residential buildings and population. In Italy, census data are produced by ISTAT [48], the National Institute of Statistics, and provide information on buildings and population at census tract level. To define inventories both for buildings and population at OMI level, ISTAT data can be associated to OMI zones based on geographical location of the census tract in each zone, determined using GIS software (QGIS 3.22). Thus, for example, residential buildings in an OMI zone are derived by summing residential buildings in all census tracts belonging to the zone.

ISTAT building typologies are identified by a combination of construction material (masonry, reinforced concrete, other), number of storeys (1, 2, 3, 4 or more storeys) and construction age (<1919, 1919–1945, 1946–1960, 1961–1970, 1971–1980, 1981–1990, 1991–2000, 2001–2005, >2005). However, at census tract level, only aggregated information on buildings is publicly available, e.g., it is possible to know how many masonry buildings there are within the census tract, but it is not possible to know how many of them have two floors and were built before 1919, or similarly how many buildings were built before 1919 but not how many are masonry buildings with two floors. Still, such disaggregated information is a crucial input for compiling building inventory for seismic risk at territorial scale. For privacy reasons, disaggregated data are available only at municipal scale. To overcome this issue, a procedure for downscaling ISTAT data at OMI zone level is presented herein. Figure 5 shows the procedure adopted herein to downscale census data.

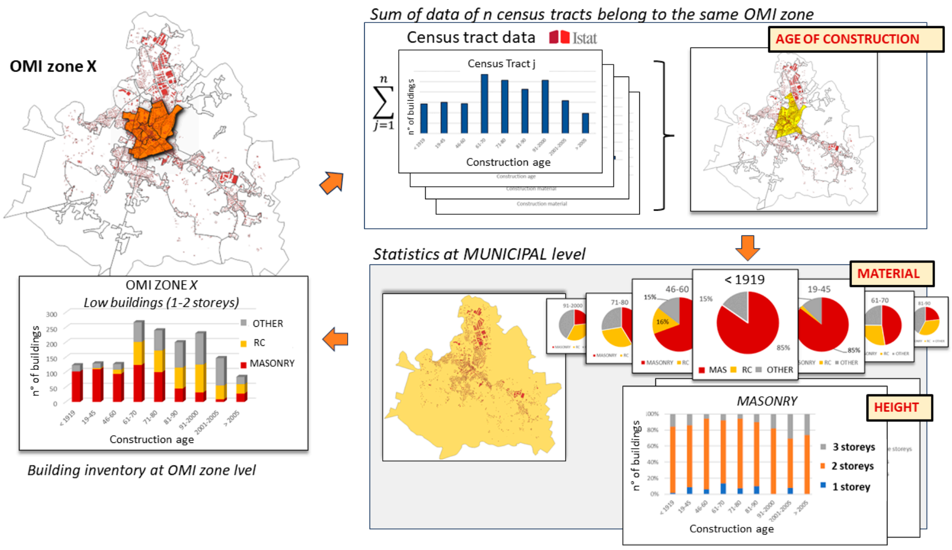

Figure 5. Downscaling of census data available at municipal level.

More specifically, for a given town, statistics at municipal level regarding construction material and construction age are also considered valid at OMI level. This means that, for example, if at municipal level 47% of buildings built between 1961 and 1970 are masonry type, at OMI level masonry buildings still represent 47% of all buildings built in the period (1961–1970). The number of buildings built in different ISTAT age ranges is derived by information available at census tract level, i.e., from the census tracts (j = 1, . . . , n) that belong to the considered OMI zone. The number of buildings with a given construction material is then obtained by adopting the percentage occurrence defined at municipal level as a function of the period of construction. Finally, for each construction material, the percentage occurrence related to classes of height, evaluated from the previously mentioned statistics also applied for each OMI zone, are used to estimate the number of buildings with 1, 2, 3, 4 or more storeys. In this way, it is possible to obtain the number of buildings in each census building typology within each OMI zone.

To define the flood exposure model, the following steps have been implemented: (1) the footprint of buildings from OpenStreetMap (OSM) were adopted and the geometrical information of the area has been added to the GIS; (2) the census information concerning the statistical distribution of buildings with number of floors equal to one, two and greater than three was distributed at the at building level within each census tract; (3) the vulnerability characteristic, that for this analysis is the building use, has been associated to each building adopting the CORINE Land Cover [49] inventory updated to 2018, that consists of an inventory of land cover in 44 classes. In the exposure model defined for the flood risk evaluation, each building from OSM is characterized by a geometrical area and a distribution of the number of storeys derived from census data. Homogeneously, at census level, the ratios between buildings with one to three or more storeys were determined, and the values of these ratios were assigned to each structure in the model, as also proposed in the HAZUS Inventory [30]. Therefore, aggregation is conducted by multiplying these variables (area and the distribution of the number of floors) for each asset and summing them at OMI scale using the GIS environment.

For the scope of the analysis, the following CORINE Land Cover classes have been considered: continuous and discontinuous urban fabric, industrial and commercial units. It is important to note that, because the aggregation at the OMI zone level (scale at which the multi-risk analysis was performed) of OSM building surfaces showed significant differences with the surface areas surveyed by ISTAT, the former was normalized to the census area. Furthermore, in order to have results comparable with those obtained from seismic risk, only residential buildings were considered for impact evaluation.

2.2.3. Vulnerability Models

Vulnerability relates to the susceptibility of assets such as objects, systems and populations exposed to disturbances, stressors or shocks as well as to the lack of capacity to cope with and to adapt to these adverse conditions [46]. Vulnerability can be divided into the following categories: physical, economic, social, institutional, environmental, agricultural and health [45]. In the scope of the present work, physical vulnerability has been considered.

In the last National Risk Assessment for Italy [47], several vulnerability models are proposed for estimating seismic risk. Among them, the models presented in [50,51] are adopted in this study. The first [50] describes seismic vulnerability of (residential) masonry buildings through empirical fragility curves. The latter expresses the probability of exceeding a given damage state as a function of PGA values using the cumulative lognormal distribution. The five damage grades of the EMS-98 scale [52] are adopted for describing global damage attained. Masonry buildings are classified into three vulnerability classes (A, B, C1 in decreasing order of vulnerability) based on their typological and structural features (e.g., irregular or regular texture of masonry, flexible or rigid diaphragms). For each class a different set of fragility curves is defined. The model for RC buildings [51] still expresses vulnerability through empirical fragility curves considering the five damage grades of the EMS-98 scale. Two vulnerability classes are defined: C2 class that includes RC building design for gravity loads only and D class that refers to RC structures with seismic design.

The downscaling procedure presented in Section 2.2.2 allows for obtaining information on census building typologies distribution at OMI zone level. In other words, in each unit of analysis the number of buildings for each combination of construction material, number of storeys and period of construction is known. Therefore, in order to use the above-mentioned fragility models for assessing the expected damages to structures, it is necessary to associate the vulnerability classes identified in the vulnerability models to the building typologies given by the census [47,53]. In [50], the authors proposed an exposure matrix that provides the percentages of census categories (class of height and period of construction) belonging to different vulnerability classes. This matrix is adopted herein, as well. On the contrary, as the two classes defined for RC buildings (C2 and D) differ only regarding the type of design (gravity loads or seismic design), the age of construction can be used as the key feature to classify buildings. This means that if a building was built before the main seismic regulations were introduced, it is considered designed for gravity loads only; on the contrary, if it was built after their introduction, it is considered seismically designed.

Direct damages caused by floods are typically assessed using flood damage curves in standard practice. These curves establish a relationship between various hazard variables, such as water depth and flood duration, and the physical consequences of different types of buildings and their contents (e.g., residential buildings and furniture, industrial buildings and machinery). The technical and scientific literature provides a wide range of methodologies for estimating damage functions, as well as established catalogues of functions (e.g., [28]). Focusing on the relationship between exposure and vulnerability, different damage curves for different vulnerability characteristics can be used, depending on the chosen vulnerability library.

For the case study, the vulnerability functions proposed in [28] were adopted. This dataset contains damage curves representing damage as a function of water depth and the corresponding maximum damage values for a variety of assets and land-use classes. The damage curves have been produced per damage class: residential, commerce, industry, agriculture, infrastructure and transport for each continent separately (Africa, Asia, North-America, South/Central-America, Oceania and Europe). The present application has adopted the curve proposed for European residential buildings.

2.2.4. Consequence Models

Consequence functions allow for evaluation of the expected impacts of hazardous events. The functions proposed in [47] are used herein to evaluate seismic risk in terms of monetary losses. Specifically, a proportion of the reconstruction cost of buildings is assigned to each damage grade of the EMS-98 scale (i.e., 2%, 10%, 30%, 60%, 100% for damage to D1 to D5, respectively). Thus, direct economic losses are calculated as a function of (1) the unit cost of a building (i.e., reconstruction cost expressed in euro/m^2), (2) the probability to experience the *i*-th damage state for the considered building typology, (3) the built-up area and (4) the percentage of replacement cost associated with the *i*-th damage state. A unit cost of 1350 euro/m^2 is adopted regardless of building typology [47]. Obviously, for risk comparison purposes the same reconstruction costs should also be adopted in estimating flood risk.

For flood evaluations, the impacts or consequences considered in the analysis derive from tangible direct damage and the population affected. The economic impact can be evaluated by multiplying the percent damage and the economic value of the considered asset. The way in which this economic value is estimated changes according to the type of exposed element. As described in [54], for buildings, it consists in the recovery and replacement costs that are the cost per unit area to be sustained to reconstruct the previous building and the cost per unit area to replace existing contents, respectively. The replacement/recovery cost assessment on one hand may rely on insurance data [55], on the other on socio-economic proxies. In the simplest case, the vulnerability function for population is just a “affected/not affected” binary function, which considers the population located inside the flooded area as affected. A further detail allows classifying affected people into different hazard zones. Four hazard zones (very high, high, moderate, low flood hazard) can be defined based on the human instability in floodwaters using available literature [56–58] together with expert judgments. When information on water velocity is not available, similar zoning classification is performed only on the basis of water depth information.

3. Results and Discussion

Figure 6 shows the values of EAL per square meter at municipal level for the area under investigation, obtained by adding EALs of municipality’s OMI zones. As expected, earthquake potential losses/m^2 are higher in municipalities located in the north-west part of the study area. Concerning the flood, the economic losses are concentrated in the north-west and in the south of the selected municipalities, since in these parts the flooded area is more extensive compared to others, with the highest values of water depth (Figure 3a).

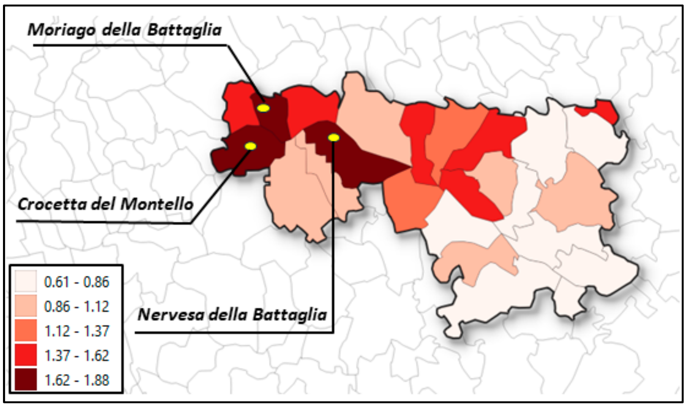

(**a**)

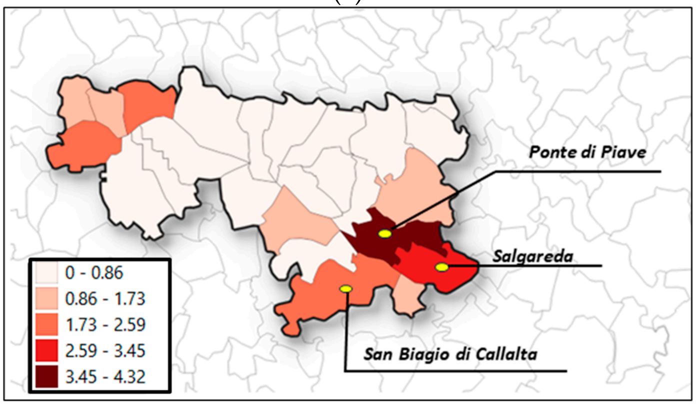

(**b**)

Figure 6. Values of EAL/m^2 due to earthquake (**a**) and due to flood (**b**) in the municipality of the study area.

The town of Crocetta del Montello shows the highest value of such losses (1.87 euro/m^2), followed by Moriago della Battaglia (1.8 euro/m^2) and Nervesa della Battaglia (1.7 euro/m^2). The OMI zones classified as E1 suburb area) and R1 (extra-urban areas) are the most affected by seismic impacts in Crocetta del Montello and E1 in Moriago della Battaglia. As a matter of fact, a significant portion of buildings in those areas belong to the most vulnerable class A (36% in Crocetta del Montello and the 25% in Moriago della Battaglia), versus the low percentages of buildings in such class in the other zones (Figure 7). In Nervesa della Battaglia, the extra-urban area (R1) shows the highest value of losses per square meter, due to the prevalence of exposed buildings belonging to class A and class B (43% vs. 32% in the B1 zone and the 28% in the E1 zone).

For the flood, in the southern part, there is an overlap with a greater presence of residential and industrial/commercial construction, leading to higher losses. Ponte di Piave, Salgareda and San Biagio di Callalta present higher values of EAL/m^2 (4.32 euro/m^2, 2.77 euro/m^2 and 1.96 euro/m^2, respectively). In Ponte di Piave, the OMI zone showing highest result is the central area B1 (7.81 euro/m^2), but this value is also significant in R1 (4.39 euro/m^2) and E2 zones (2.11 euro/m^2). In Salagareda, all zones present a value of EAL/m^2 between 2.5 and 5 euro/m^2, except for the E2 area.

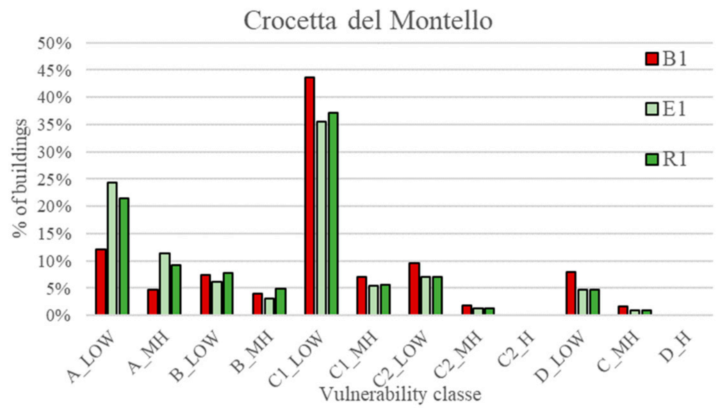

(**a**)

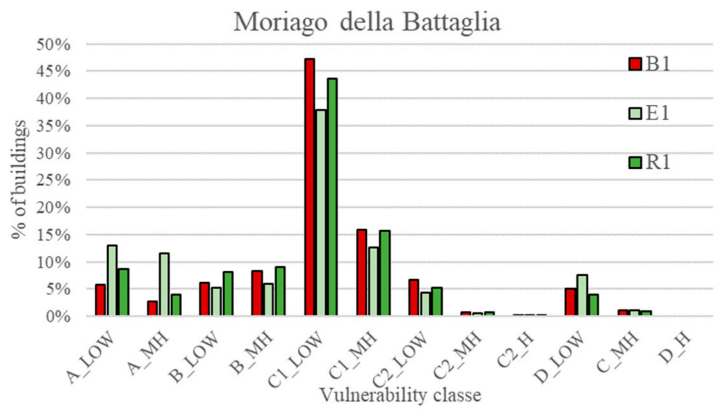

(**b**)

Figure 7. Inventory comparison for the municipality of Crocetta del Montello (**a**) and Moriago della Battaglia (**b**).

Figure 8 shows the ratios between EAL due to flood and EAL due to earthquake for each municipality analyzed. When this ratio is greater than 1, it means that flood risk predominantly effects the municipality. For instance, in the municipalities of Ponte di Piave, Salgareda and San Biagio di Callalta, potential losses caused by flood in the considered time frame (1 years) could be much higher that seismic ones with EALs ratios of 5.78, 4.13 and 3.22, respectively.

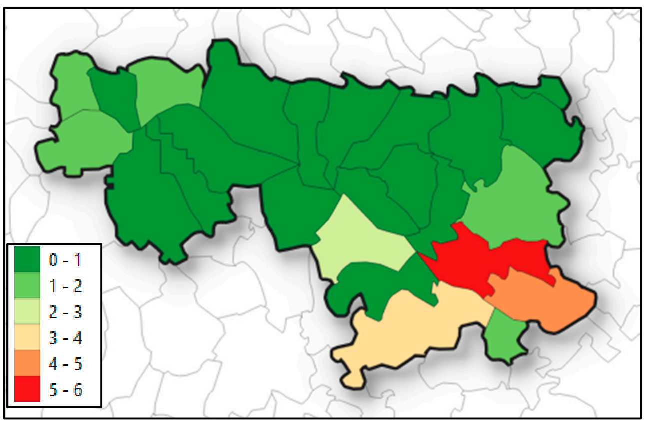

Figure 8. Map of the ratios between flood EAL and seismic EAL at municipal level.

Figure 9 shows the risk curves for OMI zone B1 of the city Ponte di Piave, where the EALs ratio is the highest (11.5). In the figure are also shown: risk curves for OMI zone

E3 of the city of Breda di Piave (EALs ratio = 3), where flood risk is slightly higher than flood risk (Figure 9b); risk curves for OMI zone B1 of Zeson di Piave (EALs ratio = 0.77), where seismic risk is slightly higher than flood risk (Figure 9c); and risk curves for OMI zone E2 of Maserada sul Piave (EALs ratio = 1.13) where the two risks assume very similar values in terms of EAL/m^2 (Figure 9d). It is worth noting that EALs ratio at municipal level could change greatly when considering single OMI zones. As a matter of fact, Breda di Piave has medium–low ratio at municipal level (EALs ratio = 0.91, see also Table 1) but focusing on single OMI zones it can be observed that despite flood hazard being completely absent in most of them, in the area where such hazard is present the related risk could be very relevant (in the E3 zone, flood EAL is three times that of seismic EAL). This is due to the proximity to the Piave river to the E3 zone. In Zeson di Piave, the urban settlement (corresponding to OMI zone B1) is located at such a distance from the banks of the Piave river that it is not significantly affected by its potential inundation and, therefore, expected losses are mostly caused by earthquakes. However, in zone R1 of the same city (Zeson di Piave), flood impacts may be more relevant (EALs ratio = 2.26). Similarly, despite EAL due to flood and EAL due to earthquakes assuming similar values in zone E2 of Maserada sul Piave, as only few buildings are expected to be affected by flood and seismic hazard is medium-low intensity, in zone R1 of the municipality, flood risk could be three times greater than seismic (EALs ratio = 3.24), while in other zones it is completely absent (i.e., no area is expected to be flooded). On the contrary, in Ponte di Piave, flood risk tends to be much higher than seismic risk in the whole municipal territory (EALs ratio > 2.6 in all OMI zones). Such results demonstrate the notable spatial variability of flood hazards and the key role played by the knowledge of buildings' spatial distribution within each territorial unit of analysis for a proper estimation of flood impacts.

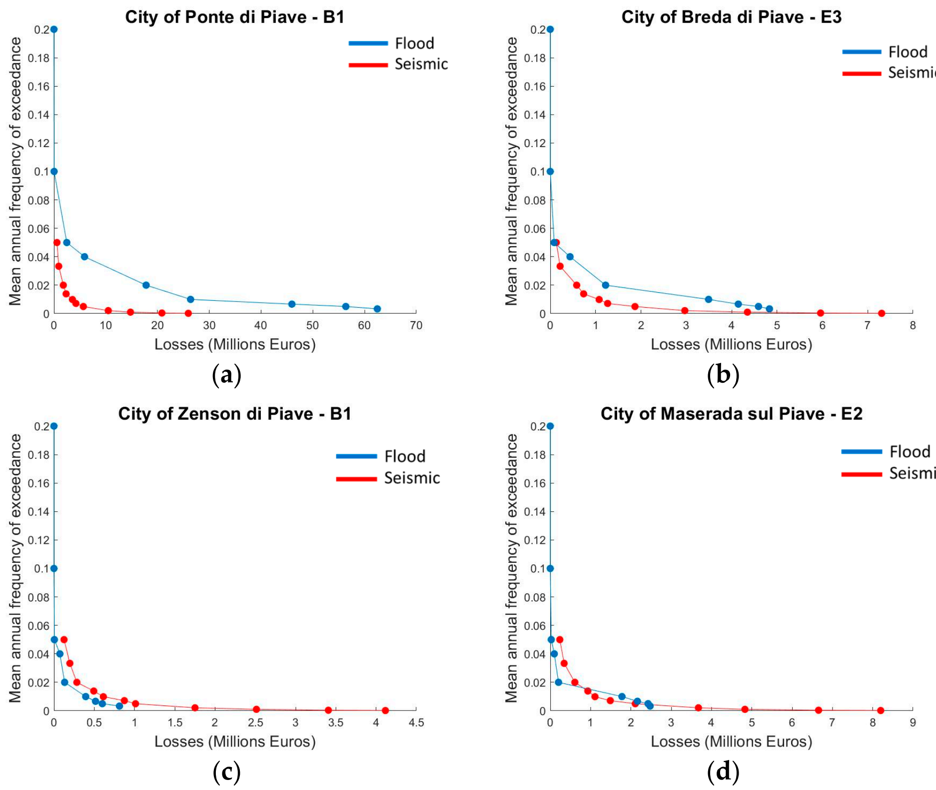

Figure 9. Risk curves for OMI zone B1 of the city of Ponte di Piave (**a**), for OMI zone E3 of the city of Breda di Piave (**b**), for OMI zone B1 of the city of Zenon di Piave (**c**) and for OMI zone E2 of Maserada sul Piave (**d**).

Table 1. Values of EAL due to earthquake (EAL seismic), flood (EAL flood) and both hazards (multi-risk EAL). The value of EAL/m^2 and the ratio between flood and seismic EAL are also reported.

Municipality	EAL Seismic (EUR)	EAL/m^2	EAL Flood (EUR)	EAL/m^2	Multi-Risk_EAL	EAL/m^2	RATIO
Ponte di Piave	262,570	0.75	1,517,601	4.32	1,780,171	5.06	5.78
Crocetta del Montello	531,580	1.88	549,450	1.94	1,081,030	3.82	1.03
Salgareda	184,992	0.67	764,303	2.77	949,294	3.44	4.13
Sernaglia della Battaglia	418,481	1.41	537,705	1.82	956,185	3.23	1.28
Moriago della Battaglia	234,297	1.81	174,396	1.35	408,693	3.16	0.74
Vidor	246,553	1.42	256,490	1.48	503,043	2.90	1.04
San Biagio di Callalta	306,002	0.61	985,664	1.96	1,291,666	2.57	3.22
Oderzo	984,482	1.11	1,295,806	1.46	2,280,288	2.56	1.32
Cimadolmo	234,545	1.51	127,395	0.82	361,940	2.33	0.54
Maserada sul Piave	290,981	0.75	602,254	1.54	893,235	2.29	2.07
Portobuffolè	61,318	1.57	27,272	0.70	88,589	2.27	0.44
Zenson di Piave	64,729	0.81	114,069	1.43	178,798	2.25	1.76
Nervesa della Battaglia	606,172	1.71	114,598	0.32	720,771	2.03	0.19
Susegana	572,677	1.10	434,121	0.84	1,006,798	1.94	0.76
Spresiano	543,945	1.13	285,293	0.59	829,238	1.72	0.52
Breda di Piave	299,809	0.88	272,680	0.80	572,489	1.67	0.91
Vazzola	473,128	1.51	17,651	0.06	490,779	1.57	0.04
Santa Lucia di Piave	545,338	1.44	7253	0.02	552,591	1.46	0.01
Mareno di Piave	483,423	1.15	15,611	0.04	499,034	1.19	0.03
Ormelle	165,597	0.84	52,777	0.27	218,374	1.11	0.32
San Polo di Piave	236,634	1.08	2727	0.01	239,361	1.09	0.01
Fontanelle	212,167	0.77	88,371	0.32	300,538	1.08	0.42
Giavera del Montello	229,634	1.05	0	0.00	229,634	1.05	0.00
Mansuè	185,164	0.85	42,759	0.20	227,923	1.04	0.23
Volpago del Montello	461,205	1.03	0	0.00	461,205	1.03	0.00

Table 1 reports the values of EAL obtained for each municipality in the study area and the ratios between seismic and flood EALs. The value of multi-risk EAL, given by the sum of EAL due to earthquakes and EAL due to floods, is also reported. The towns of Crocetta del Montello, Salgareda and Moriago della Battaglia show very high multi-risk EAL/m^2, consistently with preliminary results obtained by adopting the index-based procedure (RI = 0.48, RI = 0.58, RI = 0.48, respectively, as also shown in Figure 1). Medium–high multi-risk EAL/m^2 are obtained in Sernaglia della Battaglia, Vidor and Zenson di Piave where medium–high RI values were estimated as well (RI = 0.42; RI = 0.34; RI = 0.45, respectively). In Cimaldomo (RI = 0.48), Portobuffolè (RI = 0.69) and Nervesa della Battaglia (RI = 0.53) the preliminary approach for case study identification slightly overestimates the risk level. This is probably due to an overestimation of flood risk. For instance, in Cimaldomo the percentage of expected flooded area is approximately 62% of the entire municipal territory; however, by observing the footprint of buildings in the flooded area (used for the quantitative risk estimation) it can be noted that most of it is not covered by residential buildings. The low percentage of buildings in exposed areas leads to a medium–low value of flood expected impacts (flood EAL/m^2 = 0.82) and medium–high value of total EAL/m^2 (2.33). The main differences between the results of the two approaches (semi-quantitative and quantitative risk assessment) can be observed for the city of Ponte di Piave (RI = 0.23). Unlike the previous mentioned cases, in Ponte di Piave flood risk is significantly underestimated in the preliminary assessment. Despite the percentage of expected flooded area being quite high (about 70%), almost 100% of municipal buildings fall into the area. Similar but less significant discrepancies can be observed for the town of Susegana (RI = 0.12).

Such comparisons underline some potential limitation of the index-based approach adopted in assessing flood risk. It is worth mentioning that some discrepancies in risk estimation may be also due to the choice of hazard/vulnerability model adopted. For instance, the choice of the hazard input (e.g., flood maps providing the extension of the flooded area for a specific return period) may affect the RI value obtained [24]. Nevertheless, results obtained highlighted a good performance of the risk index adopted for the identification of the multi-risk hotspot.

4. Conclusions

This study presents an application of the multi-layer single risk assessment in Italy. Specifically, the methodology proposed within the BORIS project [21] for the harmonization of seismic and flood risk assessment procedures is adopted herein. The index-based approach developed in [24] is used for a preliminary semi-quantitative multi-risk evaluation. This evaluation allowed identifying of areas most affected by potential impacts of earthquakes and floods within the Veneto region. Based on such results, the study area for the current application is selected. Unlike the applications presented in the (BORIS) project [41] where the assessment is performed at municipal level, a lower scale of analysis is used herein, namely, the OMI zone level. Such a territorial scale is suitable for dividing urban areas in homogeneous zones accounting for building's typologies and buildings' state of preservation. Moreover, as buildings' market values are also considered for their identification and delimitation, the OMI zones can also be considered as homogeneous areas for socio-economic conditions, allowing for an easy integration of such parameters into the risk evaluation process [59]. The comparison between the two risks is performed in terms of direct economic losses both at municipal level and at OMI zone level. This multi-scale approach enables detection of (1) the municipalities where one (or both) hazard may lead to significant monetary losses (the metric used in this study) and (2) to deepen the analysis investigating in which municipal area (i.e., OMI zone) expected losses are particularly high. Thus, this approach represents a useful tool to compare and rank risks and for the detection of areas that mostly need mitigation actions against one or more risks.

This methodology is also versatile as it could easily be implemented in any other international context of interest, regardless of their geographic and demographic features and the impending hazards considered. Potential challenges in applying it in other areas may be related to the availability of data. In fact, as also observed in [60,61], census data in different countries may be available at very large resolution and may provide very limited data on buildings. For example, in Austria, the AGWR (Building and Housing Register of Statistics Austria) does not provide data regarding the construction material for up to 80% of residential buildings. In such a case, alternative sources of information that provide building information at larger scale may be adopted for compiling building inventory, such as [62]. The issue related to the lack of data could also be more relevant when a small scale of analysis is adopted (e.g., the OMI zone). In the application of the approach considering other impending hazards, it is important to select assets for the analysis and metrics for multi-risk evaluation consistently with the scope of the assessment. For instance, if the aim of the analysis is the estimation of shelter demand, people would be the asset to be considered at risk and impacts would be estimated in terms of homelessness (i.e., displaced people due to unusability of buildings caused by their structural/non-structural damages as well as the lack of services in the utilities). In this study, the comparison of seismic and flood risks in terms of direct economic losses (due to buildings structural damages) is meant to be used as support for the definition of preparedness and response actions. Regarding preparedness purposes, it allows for understanding the highest risk to be faced in the area of interest and what the total level of losses expected would be when the two risks occur within a short space of time. This could be useful for estimating insurance cover premium rates as well. Regarding response planning, it could also be used to understand which area should be avoided in the selection of earthquake emergency shelter sites (as potentially hit by floods).

It is worth mentioning that the analysis of only residential buildings, carried out in this study, may lead to inaccurate estimation of potential (economic) losses. Besides residential buildings, other types of structures also contribute, such as public buildings and infrastructures and cultural heritage sites. Moreover, as observed in [63] about the economic losses due of earthquakes, the cost related to the interruption of productive activities (involving commercial/industrial buildings) and the cost of emergency management may be quite significant in some cases; however, the costliest actions are related to the repair and strengthening interventions for private buildings, which in some cases may reach 60% of the total costs for earthquakes. In the case of floods, damage to buildings caused by floods may be less relevant than impacts in terms of indirect economic losses, i.e., losses caused by business disruption. For this reason, commercial and industrial buildings should also be considered in the analysis. However, given the level of details and amount of data required for consistent evaluation of risk for such types of structures (commercial/industrial), both in terms of direct and indirect economic losses, these assets are often neglected in risk evaluations. Future studies should also address these issues taking into account the availability and accessibility of exposure data.

It is also important to mention that results of the application presented herein may also be improved through the integration of socio-economic dimensions. In fact, parameters such as older age and poverty may increase population susceptibility to disasters. Beyond the increased number of social impacts (i.e., deaths, injuries) due to mobility, health and communication issues, low-income people may also tend to experience the largest economic impacts [64]. Therefore, with the aim of helping decision makers in selecting the most suitable mitigation options as well as the priority of actions, it could also be useful to account for different social groups in estimating impacts [59,65].

Author Contributions: Formal analysis, G.T. and D.O.; Writing—original draft, G.T. and D.O.; Writing—review & editing, N.R. and M.P.; Supervision, N.R. and M.P. All authors have read and agreed to the published version of the manuscript.

Funding: The CO-FRAME_NA project "Comprehensive multi-hazard & multirisk Framework_Napoli" (2021–2023) has received funding from the University of Napoli Federico II (UNINA) within the FRA 2020 Programme (Finanziamento Ricerca di Ateneo, D.R. n. 2449, 21 July 2020). It is coordinated by the UNINA Department of Architecture (DiARC) and involves as partners the Department of Social Sciences (DiSS) and the Department of Structures for Engineering and Architecture (DiSt).

Institutional Review Board Statement: Not applicable.

Informed Consent Statement: Not applicable.

Data Availability Statement: The data presented in this study are available on request from the corresponding author. The data that support the findings of this study are not publicly available as subjected to third party restrictions.

Acknowledgments: CIMA Research Foundation wants to thank GENERALI S.p.A. for allowing the use of the flood hazard maps that were jointly developed.

Conflicts of Interest: The authors declare no conflict of interest.

References

1. UNISDR. *United Nations Office for Disaster Risk Reduction: 2018 Annual Report*; UNISDR: New York, NY, USA, 2018.
2. Marzocchi, W.; Mastellone, M.; Di Ruocco, A. Principles of Multi-Risk Assessment: Interactions Amongst Natural and Man-Induced Risks. European Commission, 2009. Available online: http://cordis.europa.eu/documents/documentlibrary/106097581EN6.pdf (accessed on 1 September 2022).
3. de Ruiter, M.C.; Couasnon, A.; van den Homberg, M.J.; Daniell, J.E.; Gill, J.C.; Ward, P.J. Why We Can No Longer Ignore Consecutive Disasters. *Earth's Futur.* **2020**, *8*, e2019EF001425. [CrossRef]
4. Satake, K. Advances in earthquake and tsunami sciences and disaster risk reduction since the 2004 Indian ocean tsunami. *Satake Geosci. Lett.* **2014**, *1*, 15. [CrossRef]
5. LeComte, D. International Weather Highlights 2018: Winter Storms, Blistering Heat Waves, Japan's Summer of Extremes. *Weatherwise* **2019**, *72*, 24–31. [CrossRef]
6. Cotti, D.; Harb, M.; Hadri, A.; Aboufirass, M.; Chaham, K.R.; Libertino, A.; Campo, L.; Trasforini, E.; Krätzschmar, E.; Bellert, F.; et al. An Integrated Multi-Risk Assessment for Floods and Drought in the Marrakech-Safi Region (Morocco). *Front. Water* **2022**, *4*, 886648. [CrossRef]

7. United Nations Office for the Coordination of Humanitarian Affairs (OCHA). Syrian Arab Republic: Earthquakes—Syria Situational Updates No. 6—As of 4 April 2023. 2023. Available online: https://reliefweb.int/report/syrian-arab-republic/syrian-arab-republic-earthquakes-syria-situational-updates-no-6-4-april-2023 (accessed on 16 June 2023).
8. Carpignano, A.; Golia, E.; Di Mauro, C.; Bouchon, S.; Nordvik, J. A methodological approach for the definition of multi-risk maps at regional level: First application. *J. Risk Res.* **2009**, *12*, 513–534. [CrossRef]
9. Delmonaco, G.; Margottini, C.; Spizzichino, D. *Report on New Methodology for Multi-Risk Assessment and the Harmonisation of Different Natural Risk Maps*; Deliverable 3.1; ARMONIA: Tokyo, Japan, 2006.
10. Zuccaro, G.; De Gregorio, D.; Leone, M.F. Theoretical model for cascading effects analyses. *Int. J. Disaster Risk Reduct.* **2018**, *30*, 199–215. [CrossRef]
11. Luino, F. Sequence of instability processes triggered by heavy rainfall in the northern Italy. *Geomorphology* **2005**, *66*, 13–39. [CrossRef]
12. Van Westen, C.J.; Quan Luna, B.; Vargas Franco, R.D. Development of training materials on the use of geo—Information for multi—Hazard risk assessment in a mountainous environment. In *Mountain Risks: Bringing Science to Society, Proceedings of the Mountain Risks International Conference, Firenze, Italy, 24–26 November 2010*; Malet, J.-P., Glade, T., Casagli, N., Eds.; CERG: Strasbourg, France, 2010; pp. 469–475; ISBN 2-95183317-1-5.
13. European Commission. Risk Assessment and Mapping Guidelines for Disaster Management. In *European Commission Staff Working Paper*; European Union: Maastricht, The Netherland, 2011.
14. Zaghi, A.E.; Padgett, J.E.; Bruneau, M.; Barbato, M.; Li, Y.; Mitrani-Reiser, J.; McBride, A. Establishing Common Nomenclature, Characterizing the Problem, and Identifying Future Opportunities in Multihazard Design. *J. Struct. Eng.* **2016**, *142*, H2516001. [CrossRef]
15. Westen, C.; Greiving, S. Environmental Hazards Methodologies for Risk Assessment and Management. In *Envionrmental Hazards Methodologies for Risk Assessment and Management*; Dalezios, N.R., Ed.; International Water Institute (IWA) Publishing: London, UK, 2017.
16. Kappes, S.; Keiler, M.; Von Elverfeldt, K.; Glade, T. Challenges of analysing multi-hazard risk: A review. *Nat. Hazards* **2012**, *64*, 1925–1958. [CrossRef]
17. Marzocchi, W.; Garcia-Aristizabal, A.; Gasparini, P.; Mastellone, M.L.; Di Ruocco, A. Basic principles of multi-risk assessment: A case study in Italy. *Nat. Hazards* **2012**, *62*, 551–573. [CrossRef]
18. Iannacone, L.; Gentile, R.; Galasso, C. Simulating interacting multiple natural-hazard events for lifecycle consequence analysis. In Proceedings of the 14th International Conference on Applications of Statistics and Probability in Civil Engineering, ICASP14, Dublin, Ireland, 9–13 July 2023.
19. Otárola, K.; Iannacone, L.; Gentile, R.; Galasso, C. A Markovian framework for multi-hazard life-cycle consequence analysis of deteriorating structural systems. In Proceedings of the 14th International Conference on Applications of Statistics and Probability in Civil Engineering, ICASP14, Dublin, Ireland, 9–13 July 2023.
20. Zschau, J. Where Are We with Multihazards, Multirisks Assessment Capacities? 2017. Available online: https://drmkc.jrc.ec.europa.eu/ (accessed on 13 January 2023).
21. Polese, M.; Tocchi, G.; Babič, A.; Dolsek, M.; Faravelli, M.; Quaroni, D.; Borzi, B.; Rebora, N.; Ottonelli, D.; Wernhart, S.; et al. Multi-risk assessment in transboundary areas: A shared framework for harmonized evaluation considering seismic and flood risks. *Int. J. Disaster Risk Reduct.* 2023, *submitted for publication*.
22. EM-DAT. EM-DAT: The International Disaster Database. 2008. Available online: http://www.emdat.be/Database/Trends/trends.html (accessed on 16 January 2023).
23. de Ruiter, M.C.; de Bruijn, J.A.; Englhardt, J.; Daniell, J.E.; de Moel, H.; Ward, P.J. The Asynergies of Structural Disaster Risk Reduction Measures: Comparing Floods and Earthquakes. *Earth's Futur.* **2020**, *9*, e2020EF001531. [CrossRef]
24. Tocchi, G.; Cremen, G.; Galasso, C.; Polese, M. Development of a multi-risk index for Italy: A tool for supporting informed decision making on disaster risk reduction prioritization. In Proceedings of the 14th International Conference on Applications of Statistics and Probability in Civil Engineering, ICASP14, Dublin, Ireland, 9–13 July 2023.
25. Stucchi, M.; Akinci, A.; Faccioli, E.; Gasperini, P.; Malagnini, L.; Meletti, C.; Montaldo, V.; Valensise, G. Mappa di Pericolosità Sismica del Territorio Nazionale 2004. Available online: http://zonesismiche.mi.ingv.it/documenti/rapporto_conclusivo.pdf (accessed on 1 July 2022). (In Italian)
26. Stucchi, M.; Meletti, C.; Montaldo, V.; Crowley, H.; Calvi, G.M.; Boschi, E. Seismic Hazard Assessment (2003–2009) for the Italian Building Code. *Bull. Seism. Soc. Am.* **2011**, *101*, 1885–1911. [CrossRef]
27. Lagomarsino, S.; Giovinazzi, S. Macroseismic and mechanical models for the vulnerability and damage assessment of current buildings. *Bull. Earthq. Eng.* **2006**, *4*, 415–443. [CrossRef]
28. Huizinga, H.; de Moel, H.; Szewczyk, W. *Global Flood Depth-Damage Functions—Methodology and the Database with Guidelines*; Joint Research Centre: Maastricht, The Netherland, 2017. [CrossRef]
29. Gentile, R.; Cremen, G.; Galasso, C.; Jenkins, L.T.; Manandhar, V.; Menteşe, E.Y.; Guragain, R.; McCloskey, J. Scoring, selecting, and developing physical impact models for multi-hazard risk assessment. *Int. J. Disaster Risk Reduct.* **2022**, *82*, 103365. [CrossRef]
30. FEMA. *Hazus 5.1, Hazus Flood Technical Manual*; Federal Emergency Management Agency: Washington, DC, USA, 2022.

31. JRC. *Guidance for Recording and Sharing Disaster Damage and Loss Data. Towards the Development of Operational Indicators to Translate the Sendai Framework into Action*; EU Expert Working Group on Disaster Damage and Loss Data; JRC: Maastricht, The Netherland, 2015.
32. Simmons, D.; Dauwe, R.; Gowland, R.; Gyenes, Z.; King, A.; Riedstra, D.; Schneiderbaue, S. *Understanding Disaster Risk: Risk Assessment Methodologies and Examples, Science for Disaster Risk Management 2017—Knowing Better and Losing Less*; Poljanšek, K., Ed.; European Union: Maastricht, The Netherland, 2017; pp. 36–131.
33. GRS. *National Disaster Risk Assessment, Version 2.0*; Government of the Republic of Slovenia: Ljubljana, Slovenia, 2018. (In Slovenian)
34. AFAD. *National Disaster Risk Assessment Report of Turkey*; Republic of Turkey—Ministry of Interior, Disaster and Emergency Management Authority: Dumlupinar, Turkey, 2019.
35. Duijm, N.J. Recommendations on the use and design of risk matrices. *Saf. Sci.* **2015**, *76*, 21–31. [CrossRef]
36. UNDRO. *Natural Disasters and Vulnerability Analysis: Report of Expert Group Meeting, 9–12 July 1979*; Office of the United Nations Disaster Relief Coordinator: New York, NY, USA, 1980.
37. Cardona, O. Estudios de vulnerabilidad y evaluación del riesgo sísmico: Planificación física y urbana en áreas propensas. *Boletín Técnico Asoc. Colomb. Ing. Sísmica* **1986**, *33*, 32–65.
38. Velásquez, C.A.; Cardona, O.D.; Mora, M.G.; Yamin, L.E.; Carreño, M.L.; Barbat, A.H. Hybrid loss exceedance curve (HLEC) for disaster risk assessment. *Nat. Hazards* **2014**, *72*, 455–479. [CrossRef]
39. Grünthal, G.; Thieken, A.; Schwarz, J.; Radtke, K.; Smolka, A.; Merz, B. Comparative Risk Assessments for the City of Cologne—Storms, Floods, Earthquakes. *Nat. Hazards* **2006**, *38*, 21–44. [CrossRef]
40. Fleming, K.; Parolai, S.; Garcia, A.; Tyagunov, S.; Vorogushyn, S.; Kreibich, H.; Mahlke, H. Harmonizing and comparing single-type natural hazard risk estimations. *Ann. Geophys. Ann. Geofis.* **2016**, *59*, S0216. [CrossRef]
41. BORIS. Deliverable D5.1: Seismic Risk, Flood Risk and Multi-Risk Assessment at Pilot Cross-Border Sites. 2022. Available online: http://www.borisproject.eu/wp-content/uploads/2022/06/BORIS-Deliverable-D5.1.pdf (accessed on 13 January 2023).
42. Ordinanza del Presidente del Consiglio dei Ministri (OPCM). Criteria for the identification of seismic zones for the production and updating of lists of the aforementioned zones. 2006. Ordinance no. 3519 of the 28th April 2006 (in Italian).
43. Mori, F.; Mendicelli, A.; Moscatelli, M.; Romagnoli, G.; Peronace, E.; Naso, G. A new Vs30 map for Italy based on the seismic microzonation dataset. *Eng. Geol.* **2020**, *275*, 105745. [CrossRef]
44. Masi, R.; Gabellani, S.; Silvestro, F.; Pignone, F.; Poletti, M.L.; Campo, L.; Trasforini, E.; Ferraris, L.; De Paola, F. Creazione di Scenari di Inondazione in Tempo Reala per Scopi di Protezione Civile in Piccoli e Medi Bacini. In Proceedings of the XXXVII Convegno Na-zionale di Idraulica e Costruzioni Idrauliche, Reggio Calabria, Italy, 7–9 September 2020; (In Italian). Available online: https://www.iat.unina.it/pdf/tesi/abstract_Rocco_Masi_LM.pdf (accessed on 25 June 2023).
45. UNISDR. Terminology on Disaster Risk Reduction. 2009. Available online: http://www.unisdr.org/we/inform/terminology (accessed on 1 December 2022).
46. Poljanšek, K.; Marín Ferrer, M.; De Groeve, T.; Clark, I. (Eds.) *Science for Disaster Risk Management 2017: Knowing Better and Losing Less*; EUR 28034 EN; Publications Office of the European Union: Luxembourg, 2017; ISBN 978-92-79-60678-6. [CrossRef]
47. Dolce, M.; Prota, A.; Borzi, B.; da Porto, F.; Lagomarsino, S.; Magenes, G.; Moroni, C.; Penna, A.; Polese, M.; Speranza, E.; et al. Seismic risk assessment of residential buildings in Italy. *Bull. Earthq. Eng.* **2021**, *19*, 2999–3032. [CrossRef]
48. ISTAT (National Institute of Statistics). 15° Censimento Generale Della Popolazione—Dati Sulle Caratteristiche Strutturale Della Popolazione, Delle Abitazioni e Variabili. 2011. Available online: http://www.istat.it/it/archivio/104317 (accessed on 10 May 2020). (In Italian)
49. CLC 2018, © European Union, Copernicus Land Monitoring Service 2021, European Environment Agency (EEA). *DRMKC Science for Disaster Risk Management 2017: Knowing Better and Losing Less*; JRC: Maastricht, The Netherland, 2017.
50. Rosti, A.; Rota, M.; Penna, A. Empirical fragility curves for Italian URM buildings. *Bull. Earthq. Eng.* **2021**, *19*, 3057–3076. [CrossRef]
51. Rosti, A.; Del Gaudio, C.; Rota, M.; Ricci, P.; Di Ludovico, M.; Penna, A.; Verderame, G.M. Empirical fragility curves for Italian residential RC buildings. *Bull. Earthq. Eng.* **2021**, *19*, 3165–3183. [CrossRef]
52. Grünthal, G. *European Macroseismic Scale*; Chaiers du Centre Européen de Géodynamique et de Séismologie: Luxembourg, 1998; Volume 15.
53. Tocchi, G.; Polese, M.; Di Ludovico, M.; Prota, A. Regional based exposure models to account for local building typologies. *Bull. Earthq. Eng.* **2022**, *20*, 193–228. [CrossRef]
54. Arrighi, C.; Rossi, L.; Trasforini, E.; Rudari, R.; Ferraris, L.; Brugioni, M.; Castelli, F. Quantification of Flood risk mitigation benefits: A building-scale damage assessment through the RASOR platform. *J. Environ. Manag.* **2018**, *207*, 92–104. [CrossRef]
55. Associazione Nazionale fra le Imprese Assicuratrici (ANIA). Danni da Eventi Sismici e Alluvionali al Patrimonio Abitativo Italiano: Studio Quantitativo e Possibili Schemi Assicurativi. Technical Report. 2011. Available online: http://www.ania.it/export/sites/default/it/pubblicazioni/monografie-e-interventi/Danni (accessed on 3 April 2023).
56. Abt, S.R.; Wittler, R.J.; Taylor, A.; Love, D.J. Human stability in a high flood hazard zone. *Water Resour. Bull.* **1989**, *25*, 881–890. [CrossRef]
57. Karvonen, R.A.; Hepojoki, H.K.; Huhta, H.K.; Louhio, A. *The Use of Physical Models in Dam-Break Analysis*; RESCDAM Final Report; Helsinki University of Technology: Helsinki, Finland, 2000; p. 9.

58. Arrighi, C.; Oumeraci, H.; Castelli, F. Hydrodynamics of pedestrians' instability in floodwaters. *Hydrol. Earth Syst. Sci.* **2017**, *21*, 515–531. [CrossRef]
59. Tocchi, G.; Cremen, G.; Galasso, C.; Polese, M. Integrating physical and social vulnerabilities in decision-making for disaster risk reduction. In Proceedings of the National Conference of the GNGTS 2023, Bologna, Italy, 7–9 February 2022.
60. BORIS Deliverable 2.1: Comparison of NRA. BORIS Project (GA. 101004882; UCPM-2020-PP-AG). 2022. Available online: https://www.borisproject.eu/wp-content/uploads/2022/06/BORIS-Deliverable-D2.1.pdf (accessed on 24 April 2023).
61. Crowley, H.; Ozcebe, S.; Baker, H.; Foulser-Piggott, R.; Spence, R. D7.2 State of the Knowledge of Building Inventory Data in Europe, 2014, NERA Deliverable,7, v3. Available online: https://www.orfeus-eu.org/other/projects/nera/NERA_D7.2.pdf (accessed on 1 April 2022).
62. Gamba, P. *Global Exposure Database: Scientific Features*; GEM Technical Report 2014-10; GEM Foundation: Pavia, Italy.
63. Dolce, M.; Di Bucci, D. Comparing recent Italian earthquakes. *Bull. Earthq. Eng.* **2017**, *15*, 497–533. [CrossRef]
64. Ritchie, H.; Rosado, P.; Roser, M. Natural Disasters. Published online at OurWorldInData.org. 2022. Available online: https://ourworldindata.org/natural-disasters (accessed on 10 January 2023).
65. Mesta, C.; Cremen, G.; Galasso, C. Urban growth modelling and social vulnerability assessment for a hazardous Kathmandu Valley. *Sci. Rep.* **2022**, *12*, 6152. [CrossRef]